

NASA TECHNICAL NOTE



NASA TN D-5531

2.1

NASA TN D-5531



LOAN COPY: RETURN TO  
AFWL (WLQ-2)  
KIRTLAND AFB, N MEX

ANALYSIS OF THE MIXING REGION FOR  
A TWO-DIMENSIONAL JET INJECTED  
AT AN ANGLE TO A MOVING STREAM

*by Willis Braun and Marvin E. Goldstein*

*Lewis Research Center*

*Cleveland, Ohio*



0132011

1. Report No. NASA TN D-5531	2. Government Accession No.	3. Recipient's Catalog No.	
4. Title and Subtitle ANALYSIS OF THE MIXING REGION FOR A TWO-DIMENSIONAL JET INJECTED AT AN ANGLE TO A MOVING STREAM		5. Report Date November 1969	6. Performing Organization Code
		8. Performing Organization Report No. E-5163	
7. Author(s) Willis Braun and Marvin E. Goldstein		10. Work Unit No. 129-01	11. Contract or Grant No.
9. Performing Organization Name and Address Lewis Research Center National Aeronautics and Space Administration Cleveland, Ohio 44135		13. Type of Report and Period Covered Technical Note	
		14. Sponsoring Agency Code	
12. Sponsoring Agency Name and Address National Aeronautics and Space Administration Washington, D.C. 20546		15. Supplementary Notes	
16. Abstract An analysis is made of the laminar and turbulent mixing of a two-dimensional jet issuing from an orifice whose two walls are parallel to the free-stream velocity but not necessarily coplanar with each other. The difference of total pressure between the jet and the stream is assumed small compared with the dynamic pressure of the stream. The results of previous inviscid analyses are used to obtain the velocity profiles in the mixing region and the thickness of the region for jets which are separated from the downstream wall and for those which are attached. Results show that, when the orifice walls are coplanar, the attached jet has higher velocities than the separated jet as it turns into the stream; therefore, the attached jet has a thinner mixing region.			
17. Key Words (Suggested by Author(s)) Injection Laminar mixing Turbulent mixing Jet		18. Distribution Statement Unclassified - unlimited	
19. Security Classif. (of this report) Unclassified	20. Security Classif. (of this page) Unclassified	21. No. of Pages 25	22. Price* \$3.00

\*For sale by the Clearinghouse for Federal Scientific and Technical Information  
Springfield, Virginia 22151

# ANALYSIS OF THE MIXING REGION FOR A TWO-DIMENSIONAL JET INJECTED AT AN ANGLE TO A MOVING STREAM

by Willis Braun and Marvin E. Goldstein

Lewis Research Center

## SUMMARY

An analysis is made of the laminar and turbulent mixing of a two-dimensional jet issuing from an orifice whose two walls are parallel to the free-stream velocity but not necessarily coplanar with each other. The difference of total pressure between the jet and the stream is assumed small compared with the dynamic pressure of the stream. The results of previous inviscid analyses are used to obtain the velocity profiles in the mixing region and the thickness of the region for jets which are separated from the downstream wall and for those which are attached. Results show that, when the orifice walls are coplanar, the attached jet has higher velocities than the separated jet as it turns into the stream; therefore, the attached jet has a thinner mixing region.

## INTRODUCTION

The flow field which results from the oblique injection of a jet into a moving stream is of considerable interest in a number of fluid mechanical devices. Among these are ground-effect machines, jet flaps, wing fans on VTOL aircraft, fuel injection systems in combustion chambers, and air curtains.

In references 1 and 2, the two-dimensional, incompressible inviscid flow of a jet from an orifice into a flowing stream is described. In reference 1, the particular configuration in which the jet separates from the leeward surface of the orifice and a constant pressure wake forms, as shown in figure 1(a) is treated. On the other hand, in reference 2 the jet is attached to the lee surface of the orifice, and the wake region does not occur. This situation is illustrated in figure 1(b).

Of course, viscous effects can be quite significant in real fluid flows. For example, since, according to the inviscid solutions, there is, in general, a jump in the velocity

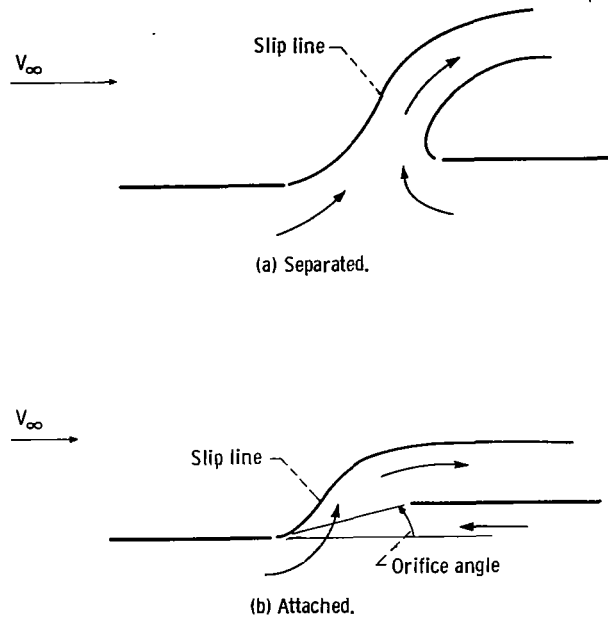


Figure 1. - Jet configurations.

across the slip line, a mixing region will be established which may be either laminar or turbulent. In the present report, the results obtained in references 1 and 2 will be used to perform an analysis of this mixing region. It will be assumed, as is usual, that the mixing region can be described by the boundary layer equations and that the external inviscid flows calculated in references 1 and 2 can be used to determine the pressure gradient in the mixing region. The effect of viscosity at the second surface of the jet (the free streamline or the downstream lip of the orifice, as the case may be) is not analyzed here.

Since the analyses in references 1 and 2 assume that the difference in the pressure between the jet and the main stream is in a certain sense (discussed more fully later) small, the same approximation will be made in the present analysis. This allows the equations for the mixing region to be integrated directly, and thus a simple closed-form solution is obtained.

## ANALYSIS

### Configuration and Notation

The notation which will be used in the analysis of the mixing region is illustrated in figure 2. The slip line  $S$  defines the boundary between the jet and the stream. The

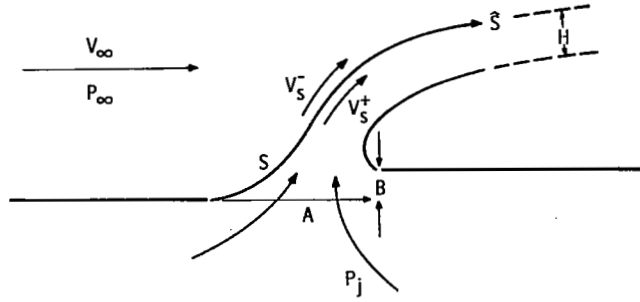


Figure 2. - Notation for mixing region analysis.

velocity of the stream along the slip line is designated  $V_S^-$ . The velocity of the jet along the slip line is, in general, not the same as  $V_S^-$  and is designated  $V_S^+$ . The distance along the slip line measured from the upstream lip of the orifice is  $\hat{S}$ . The width of the jet far from the orifice is  $H$ . The conditions which determine the boundaries of the jet and the velocities in it are the jet orifice angle,  $\tan^{-1}(B/A)$ , and the dimensionless difference of total pressures

$$\epsilon \equiv \frac{P_j - P_\infty}{\frac{1}{2} \rho V_\infty^2} \quad (1)$$

(All symbols are defined in the appendix.)

The analyses in references 1 and 2 are restricted to conditions for which  $\epsilon$  is a small parameter:

$$|\epsilon| \ll 1$$

In both of these references, the quantities  $V_S^\pm$  and  $\hat{S}$  are given to first order in  $\epsilon$  in terms of a parametric variable  $\eta$  by

$$\left[ \frac{V_S^\pm(\eta)}{V_\infty} \right]^2 = \left[ \frac{V_{S0}(\eta)}{V_\infty} \right]^2 \left[ 1 + 2\epsilon\Omega^\pm(\eta) \right] \quad (2a)$$

and

$$\hat{S} = \hat{S}_0(\eta) + \epsilon\hat{S}_1(\eta) \quad (2b)$$

The functions  $\Omega^\pm(\eta)$ ,  $\hat{S}_0(\eta)$ ,  $\hat{S}_1(\eta)$ , and  $V_{s0}(\eta)$  are given explicitly in the cited references. The velocity along the slip line when the total pressure of the jet is equal to that of the stream ( $\epsilon = 0$ ) is  $V_{s0}(\eta)$  and is the same in the stream as in the jet. The parameter  $\eta$  arises in references 1 and 2 as a coordinate in a convenient mapping and has the range  $0 \leq \eta \leq \pi$ . A useful result from references 1 and 2 for both the attached and separated jets which will be used here is that

$$\Omega^+ - \Omega^- = \frac{1}{2} \frac{V_\infty^2}{V_{s0}^2} \quad (3)$$

Viscous mixing. - According to the inviscid solution, there is, in general, a jump in the velocity across the slip line. Consequently, a mixing region will be established which may be either laminar or turbulent. For the present, laminar mixing only is considered, and subsequently the analysis is modified to apply to the turbulent case.

Let  $N$  be a coordinate normal to the slip line with positive direction into the free stream, and let  $u$  and  $v$  be the velocities in the mixing region in the  $\hat{S}$ - and  $N$ -directions, respectively. It is assumed that the boundary layer approximations for curved flow (ref. 3) hold within the mixing region. Then the equation for the momentum in the direction of the slip line is

$$u \frac{\partial u}{\partial \hat{S}} + \frac{\partial u}{\partial N} = - \frac{1}{\rho} \frac{dp}{d\hat{S}} + \nu \frac{\partial^2 u}{\partial N^2} \quad (4a)$$

and the boundary conditions for  $u$  are

$$\left. \begin{aligned} u[\hat{S}(\eta), N] &\rightarrow V_s^-(\eta) && \text{for } \sqrt{\text{Re}} N/H_0 \rightarrow +\infty \\ u[\hat{S}(\eta), N] &\rightarrow V_s^+(\eta) && \text{for } \sqrt{\text{Re}} N/H_0 \rightarrow -\infty \end{aligned} \right\} \quad (4b)$$

Equations (2a) and (4b) show that the change in velocity across the mixing region is of order  $\epsilon$ . Hence, to zeroth order in  $\epsilon$ , the velocity in the mixing region is just the zeroth order inviscid velocity. Now, according to the boundary layer assumption, variations of velocities in the  $N$ -direction in the mixing region occur over a small distance compared with the length scale for variations in the external flow. Since the normal velocity at the jet centerline is zero and the changes in velocity are of order  $\epsilon$ , the normal velocity in the mixing region can only be of order  $\epsilon$ . Hence, to within terms of

order  $\epsilon$ , the velocities  $u$  and  $v$  can be written in the form

$$u = V_{S_0} \left[ 1 + \epsilon u_1(\hat{S}, N) \right] + O(\epsilon^2) \quad (5)$$

$$v = \epsilon V_{S_0} v_1(\hat{S}, N) + O(\epsilon^2) \quad (6)$$

Now, in view of equation (2a), the boundary conditions on  $u$  are given in terms of the parametric variable  $\eta$ , whereas the differential equation for  $u$  is in terms of the variable  $\hat{S}$ . Equation (2b) allows transformation from one of these variables to the other. However, this transformation involves the small parameter  $\epsilon$ . Hence, in order to make the various orders of  $\epsilon$  explicit in the differential equation, it is convenient to make the change in variable  $\hat{S} \rightarrow \hat{S}_0$  in the equation, since the mapping  $\eta \rightarrow \hat{S}_0$  does not involve  $\epsilon$ . Thus, using equation (2b) results in

$$\begin{aligned} \left( \frac{\partial}{\partial \hat{S}} \right)_N &= \frac{dS_0}{d\hat{S}} \left( \frac{\partial}{\partial \hat{S}_0} \right)_N = \frac{1}{1 + \epsilon \frac{d\hat{S}_1}{dS_0}} \left( \frac{\partial}{\partial \hat{S}_0} \right)_N \\ &= \left( 1 - \epsilon \frac{d\hat{S}_1}{d\hat{S}_0} \right) \left( \frac{\partial}{\partial \hat{S}_0} \right)_N + O(\epsilon^2) \\ &= \left( 1 - \epsilon \frac{\frac{d\hat{S}_1}{d\eta}}{\frac{d\hat{S}_0}{d\eta}} \right) \left( \frac{\partial}{\partial \hat{S}_0} \right)_N + O(\epsilon^2) \end{aligned}$$

and

$$\left( \frac{\partial}{\partial N} \right)_{\hat{S}} = \left( \frac{\partial}{\partial N} \right)_{\hat{S}_0}$$

In view of these remarks, introducing equations (5) and (6) into the inertia terms of equation (4a) yields

$$u \frac{\partial u}{\partial \hat{S}} = V_{s0} \frac{dV_{s0}}{d\hat{S}_0} + \epsilon \left[ \frac{\partial}{\partial \hat{S}_0} \left( u_1 V_{s0}^2 \right) - \frac{d\hat{S}_1}{d\hat{S}_0} V_{s0} \frac{dV_{s0}}{d\hat{S}_0} \right] + O(\epsilon^2) \quad (7)$$

and

$$v \frac{\partial u}{\partial N} = O(\epsilon^2) \quad (8)$$

Because the static pressure is constant across the slip line, the Bernoulli equation gives the pressure gradient along the slip line as

$$\begin{aligned} -\frac{1}{\rho} \frac{dP}{d\hat{S}} &= V_s^+ \frac{dV_s^+}{d\hat{S}} \\ &= V_{s0} \frac{dV_{s0}}{d\hat{S}} + \epsilon \frac{d}{d\hat{S}} \left( \Omega^+ V_{s0}^2 \right) \\ &= V_{s0} \frac{dV_{s0}}{d\hat{S}_0} + \epsilon \left[ \frac{d}{d\hat{S}_0} \left( \Omega^+ V_{s0}^2 \right) - \frac{d\hat{S}_1}{d\hat{S}_0} V_{s0} \frac{dV_{s0}}{d\hat{S}_0} \right] + O(\epsilon^2) \end{aligned} \quad (9)$$

When equations (2a), (5), (7), (8), and (9) are substituted into equation (4a) and the boundary conditions (4b), the zeroth order terms vanish identically in equation (4a) and the boundary conditions (eq. (4b)) are satisfied by the zeroth order terms. This, incidentally, merely verifies that equations (5) and (6) were chosen in the appropriate form. The first-order terms yield

$$\frac{\partial}{\partial \hat{S}_0} \left( u_1 V_{s0}^2 \right) = \frac{\partial}{\partial \hat{S}_0} \left( \Omega^+ V_{s0}^2 \right) + \nu V_{s0} \frac{\partial^2 u_1}{\partial N^2} \quad (10a)$$

with the boundary conditions

$$\left. \begin{aligned} u_1(\hat{S}_0, N) &\rightarrow \Omega^-(\hat{S}_0) && \text{for } \sqrt{\text{Re}} N/H_0 \rightarrow +\infty \\ u_1(\hat{S}_0, N) &\rightarrow \Omega^+(\hat{S}_0) && \text{for } \sqrt{\text{Re}} N/H_0 \rightarrow -\infty \end{aligned} \right\} \quad (10b)$$

(Notice that if  $b$  is a dimensionless quantity of order one,  $\sqrt{1 + \epsilon b} = 1 + \frac{\epsilon}{2} b + O(\epsilon^2)$ .)

Taking into account the fact that  $V_{s0}$  and  $\Omega^\pm$  are independent of  $N$  permits one to write the equation of motion in the form

$$V_{s0} \frac{\partial}{\partial \hat{S}_0} \left[ V_{s0}^2 (u_1 - \Omega^+) \right] = \nu \frac{\partial^2}{\partial N^2} \left[ V_{s0}^2 (u_1 - \Omega^+) \right] \quad (11)$$

Introduce dimensionless variables  $s$  and  $K$  defined by

$$s = \int_0^{\hat{S}_0} \nu \frac{d\hat{S}_0}{V_{s0}} \quad (12)$$

and

$$K(s, N) = \frac{V_{s0}^2}{V_\infty^2} (u_1 - \Omega^+) \quad (13)$$

Then equation (10a) assumes the form of the canonical diffusion equation:

$$\frac{\partial K}{\partial s} = \frac{\partial^2 K}{\partial N^2} \quad (14a)$$

And, in view of the condition (eq. (3)), the boundary conditions (eq. (10b)) become

$$\left. \begin{aligned} K(s, N) &\rightarrow \frac{1}{2} && \text{for } \sqrt{\text{Re}} N/H \rightarrow +\infty \\ K(s, N) &\rightarrow 0 && \text{for } \sqrt{\text{Re}} N/H \rightarrow -\infty \end{aligned} \right\} \quad (14b)$$

In equation (12), the upper limit can be taken as the exact position on the slip line  $\hat{S}$  rather than its zero-order approximation  $\hat{S}_0$ , and any correction due to this interpretation of  $s$  will appear only in a subsequent equation for second-order quantities. Hence, to within an error which will appear in the next order of the system of equations for  $u$ , equation (12) can be replaced by

$$s = \int_0^{\hat{S}} \frac{\nu \, d\hat{S}_0}{V_{s0}} \quad (15)$$

The solution to the problem defined by equations (14a) and (14b), which has the correct behavior at  $s = 0$ , is

$$K(s, N) = -\frac{1}{4} \left[ 1 + \operatorname{erf} \left( \frac{N}{2\sqrt{s}} \right) \right] \quad (16)$$

or, using equations (13), (2a), and (5)

$$u = V_s^+ - \epsilon \frac{V_\infty^2}{4V_{s0}} \left[ 1 + \operatorname{erf} \left( \frac{N}{2\sqrt{s}} \right) \right] \quad (17a)$$

Finally, equations (2a) and (3) can be used to write the velocity to order  $\epsilon$  as

$$u = V_s^+ - \frac{V_s^+ - V_s^-}{2} \left[ 1 + \operatorname{erf} \left( \frac{N}{2\sqrt{s}} \right) \right] \quad (17b)$$

The second term in equation (17) is the velocity profile in the mixing region along the slip line. The profile shape is similar for all attached and separated jets, and only the velocity and length scales vary with  $\epsilon$  and orifice angle. The solution shows that  $\sqrt{s}$  is a measure of the mixing-region thickness at any station on the slip line.

Turbulent mixing. - If the mixing is turbulent, equation (10a) can be used with  $\nu$  replaced by an eddy diffusivity. Prandtl's hypothesis (ref. 4) as applied to parallel streams (ref. 5) implies that the shear stress is of the form

$$\frac{\tau}{\rho} = \kappa \hat{S} (V_s^+ - V_s^-) \frac{\partial u}{\partial N} \quad (18)$$

where  $\kappa$  is a dimensionless constant. In equation (18), the effects of curvature are assumed to be negligible. Using equations (2a), (2b), (3), and (5) in equation (18) leads to the expression

$$\frac{\tau}{\rho} = \frac{\kappa\epsilon}{2} \hat{S} \frac{V_\infty^2}{V_{s0}} \frac{\partial u}{\partial N} = \frac{\kappa\epsilon^2}{2} \hat{S}_0 V_\infty^2 \frac{\partial u_1}{\partial N} + O(\epsilon^3)$$

which appears to be of one degree higher in  $\epsilon$  than the terms retained in the equation of motion (eq. (10a)). However, it has been found experimentally (ref. 5) that, even when parallel streams move with relative velocity corresponding to  $\epsilon < 0.2$ , the mixing can still be turbulent.

In any case,  $\kappa\epsilon V_\infty S$  can easily become large compared with  $\nu$  even for very small  $\epsilon$ , which means that the stress term in the turbulent case can be even larger than in the laminar case even though it contains an extra factor of  $\epsilon$ . Hence, retaining the factor of  $\epsilon$  in this term results in, analogous to equation (10a) for viscous mixing,

$$\frac{\partial}{\partial \hat{S}_0} \left( u_1 V_{s0}^2 \right) = \frac{\partial}{\partial \hat{S}_0} \left( \Omega^+ V_{s0}^2 \right) + \frac{\kappa\epsilon}{2} \hat{S}_0 V_\infty^2 \frac{\partial^2 u_1}{\partial N^2}$$

or

$$\frac{\partial}{\partial \hat{S}_0} \left[ \frac{V_{s0}^2}{V_\infty^2} (u_1 - \Omega^+) \right] = \frac{\kappa\epsilon}{2} \hat{S}_0 \frac{V_\infty^2}{V_{s0}^2} \frac{\partial^2}{\partial N^2} \left[ \frac{V_{s0}^2}{V_\infty^2} (u_1 - \Omega^+) \right]$$

Once again, the canonical form of the diffusion equation can be obtained by introducing a new streamwise coordinate:

$$s_t \equiv \frac{\kappa\epsilon}{2} \int_0^{\hat{S}} \frac{V_\infty^2}{V_{s0}^2} \hat{S}_0 d\hat{S}_0 \quad (19)$$

The result is

$$\frac{\partial}{\partial s_t} \left[ \frac{V_{s0}^2}{V_\infty^2} (u_1 - \Omega^+) \right] = \frac{\partial^2}{\partial N^2} \left[ \frac{V_{s0}^2}{V_\infty^2} (u_1 - \Omega^+) \right]$$

which, along with the boundary conditions (eq. (10(b))), has the solution

$$u = V_s^+ - \epsilon \frac{V_\infty^2}{4V_{s0}} \left[ 1 + \operatorname{erf} \left( \frac{N}{2\sqrt{s_t}} \right) \right] \quad (20a)$$

which is the same as equation (17a) for laminar mixing with  $s$  replaced by  $s_t$ . Hence, the procedure used to obtain equation (17b) from equation (17a) can be applied to equation (20a) to yield

$$u = V_s^+ - \frac{V_s^+ - V_s^-}{2} \left[ 1 + \operatorname{erf} \left( \frac{N}{2\sqrt{s_t}} \right) \right] \quad (20b)$$

The foregoing analyses for laminar and turbulent mixing apply to both the separated and attached jets. It is only necessary to introduce the appropriate values of  $V_{s0}$  and  $\hat{S}_0$ .

Separated jet. - When the jet is separated from the lee surface, reference 1 gives the distance along the slip line to zeroth order in terms of the parametric variable  $\eta$  as

$$\frac{\hat{S}_0}{H_0} = \int_0^\eta \frac{V_\infty}{V_{s0}(\gamma)} J(\gamma) d\gamma \quad 0 \leq \eta \leq \pi \quad (21)$$

where

$$\frac{V_{s0}(\gamma)}{V_\infty} = \left| \frac{T}{T - 2\Delta + 2i\sqrt{\Delta} \sqrt{T - \Delta}} \right| \quad (22a)$$

with

$$T = -\frac{\gamma}{\sin \gamma} e^{-i\gamma} \quad (22b)$$

and

$$J(\gamma) = \frac{(1 - \gamma \cot \gamma)^2 + \gamma^2}{\pi\gamma} \quad (22c)$$

The parameter  $\Delta$  is given as a function of the orifice angle  $\tan^{-1} B/A$  in reference 1.

It follows that, for laminar flows, the modified streamwise coordinate equation (12) is given by

$$\frac{s}{H_0^2} = \frac{\nu}{H_0^2 V_\infty} \int_0^\eta \left[ \frac{V_\infty}{V_{s0}(\gamma)} \right] \frac{d\hat{S}_0}{d\gamma} d\gamma = \frac{1}{\text{Re}} \int_0^\eta \left[ \frac{V_\infty}{V_{s0}(\gamma)} \right]^2 J(\gamma) d\gamma \quad (23)$$

where

$$\frac{H_0 V_\infty}{\nu} \approx \frac{H V_\infty}{\nu} = \text{Re}$$

For turbulent flows, equations (19) and (21) yield

$$\frac{s_t}{H_0^2} = \frac{\kappa \epsilon}{2} \int_0^\eta \left[ \frac{V_\infty}{V_{s0}(\gamma)} \right]^3 \frac{\hat{S}_0(\gamma)}{H_0} J(\gamma) d\gamma \quad (24)$$

Attached jet. - In this case, reference 2 shows that the distance along the slip line is again given by equation (21) with

$$\frac{V_{s0}(\gamma)}{V_\infty} = \left| \frac{\gamma e^{-i\gamma}}{\gamma e^{-i\gamma} + \Delta \sin \gamma} \right| \quad (25)$$

and with  $J(\gamma)$  defined as in equation (22c). As before,  $\Delta$  is related to the orifice angle  $\tan^{-1}(B/A)$  by a relation given in reference 2. The modified streamwise coordinates for laminar and turbulent mixing are given by equations (23) and (24) with equation (25) substituted for  $V_{s0}/V_\infty$ .

Mixing-zone characteristics. - Equation (14a) for viscous mixing has already been noted as the canonical diffusion equation. Thus, for an observer moving along the slip line with velocity  $V_{s0}$ , the mixing region appears (with error of  $O(\epsilon)$ ) to grow by a simple diffusion process.

The thickness of the mixing region  $2\delta$  is defined by putting

$$\delta = N \quad \text{for} \quad \frac{V_s^+ - u}{V_s^+ - V_s^-} = 0.99$$

and

$$-\delta = N \quad \text{for} \quad \frac{V_s^+ - u}{V_s^- - V_s^+} = 0.99$$

Then, for laminar mixing, equation (17) shows that

$$\text{erf} \left( \frac{\delta}{2\sqrt{s}} \right) = 0.98$$

or

$$\delta = 3.29\sqrt{s} \tag{26}$$

Similarly, for turbulent mixing

$$\delta_t = 3.29\sqrt{s_t} \tag{27}$$

It can be shown using equation (17b) that if  $N < 0$ ,  $u \rightarrow V_s^+$  as  $s \rightarrow 0$  or, equivalently, as  $\hat{S}_0 \rightarrow 0$ ; and that if  $N > 0$ ,  $u \rightarrow V_s^-$  as  $s \rightarrow 0$ . Hence, at  $s = \hat{S}_0 = 0$ , there is a discontinuity in the tangential velocity of the amount  $V_s^+ - V_s^-$ . This shows that the solution (eq. (17)) satisfies the appropriate initial condition at the lip of the orifice.

The question of the third boundary condition which arises in most mixing problems (ref. 6) is not relevant for the present solution since the linearization has the effect of reducing the order of the differential equation. The significance of this development is that the displacement of the curve  $N = 0$  from the zero-order slip line is a quantity of second order in  $\epsilon$  and can be neglected in the present linearized analysis.

An easy calculation shows that, along the line  $N = 0$ ,

$$u = \frac{V_s^+ + V_s^-}{2} = V_{s0} + O(\epsilon)$$

## RESULTS AND DISCUSSION

Equation (17b) shows that the dimensionless velocity profiles in the laminar mixing region are given by a single universal function of the variable  $N/(2\sqrt{s})$ , whereas equation (20b) shows that the dimensionless velocity profiles in a turbulent mixing region are given by the same universal function of the variable  $N/(2\sqrt{s_t})$ . This function is plotted in figure 3. The laminar and turbulent mixing-region thicknesses ( $\delta$  and  $\delta_t$ , re-

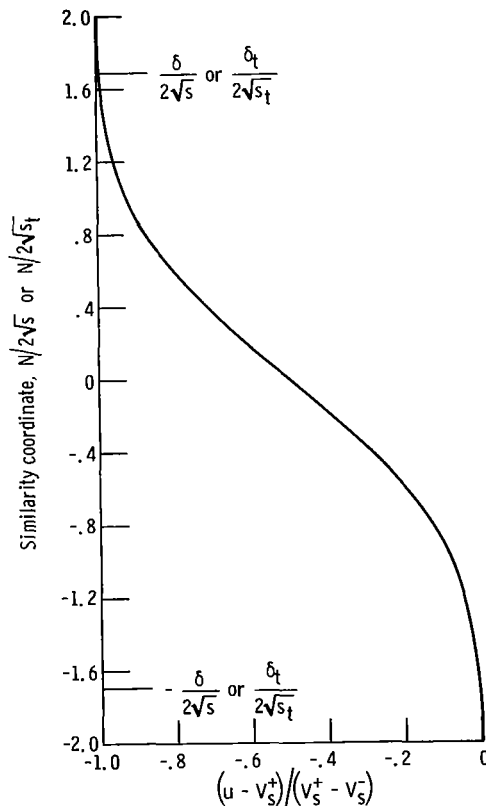


Figure 3. - Relative velocity between mixing region and jet.

spectively are defined to be the normal distance from the mixing-region centerline at which the velocity difference  $V_s^+ - u$  for  $N > 0$  (or  $V_s^- - u$  for  $N < 0$ ) has reached 99 percent of its free-stream value. The thicknesses  $\delta$  and  $\delta_t$  are given in terms of the laminar modified coordinate function  $s$  and the turbulent modified coordinate function  $s_t$ , respectively, by equations (26) and (27). The normalized values of  $\delta$  and  $\delta_t$  are also shown in figure 3. Notice that the velocity at  $N = 0$  is equal to the average of the velocities which occur at the edges of the mixing region.

The results presented in figure 3 can be used to determine the mixing-region velocity profiles and thicknesses as a function of the distance along the mixing-region centerline  $\hat{S}$  once the modified coordinate functions  $s$  and  $s_t$  are known in terms of this distance. The functional relation between  $s$  (or  $s_t$ ) and  $\hat{S}$  depends on the particular jet configuration. Thus, for the separated jet,  $s$  and  $s_t$  are given parametrically in terms of  $\hat{S}$  by equations (21) to (24). (See discussion preceding eq. (15).) For the attached jet,  $s$  and  $s_t$  are given as parametric functions of  $\hat{S}$  by equations (21), (22c), (23), and (24) with equation (25) substituted for  $V_{s0}/V_\infty$ . These equations were used to calculate  $s$  and  $s_t$  as a function of  $\hat{S}$ . The complex quantities were calculated by performing complex arithmetic on a digital computer.

The laminar modified coordinate  $s$  is given as a function of distance  $\hat{S}$  in figure 4 and 5 for the separated and attached jets, respectively. The turbulent modified coordi-

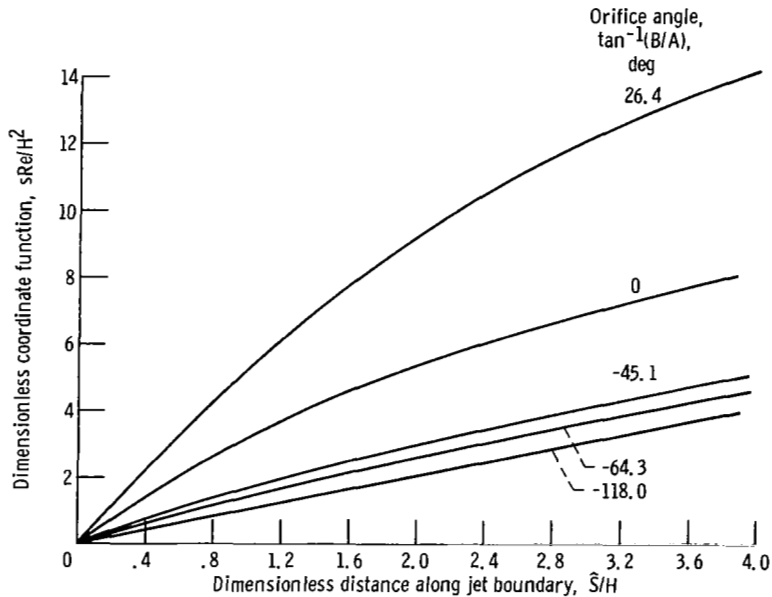


Figure 4. - Coordinate function for laminar mixing of stream and separated jet.

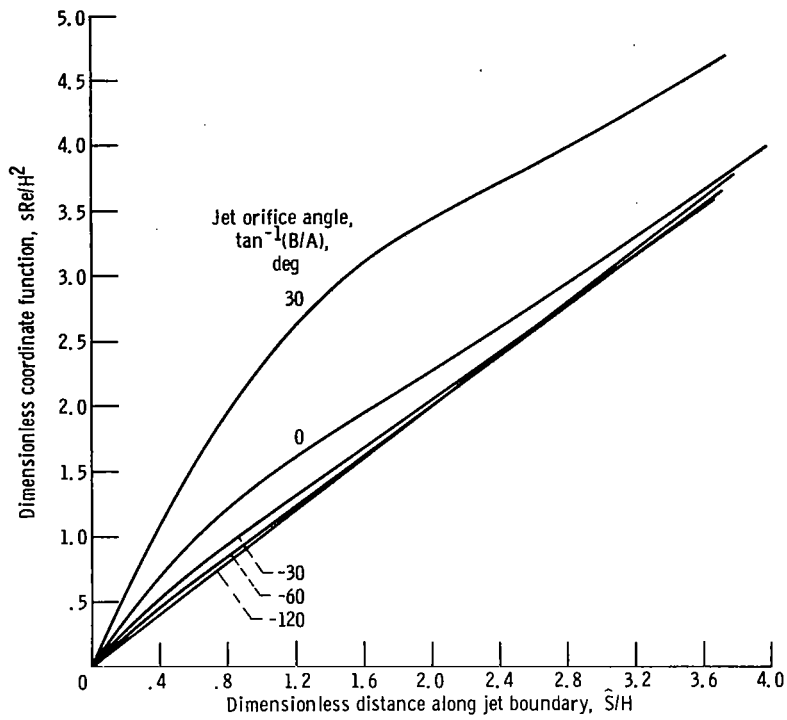


Figure 5. - Coordinate function for laminar mixing of stream and attached jet.

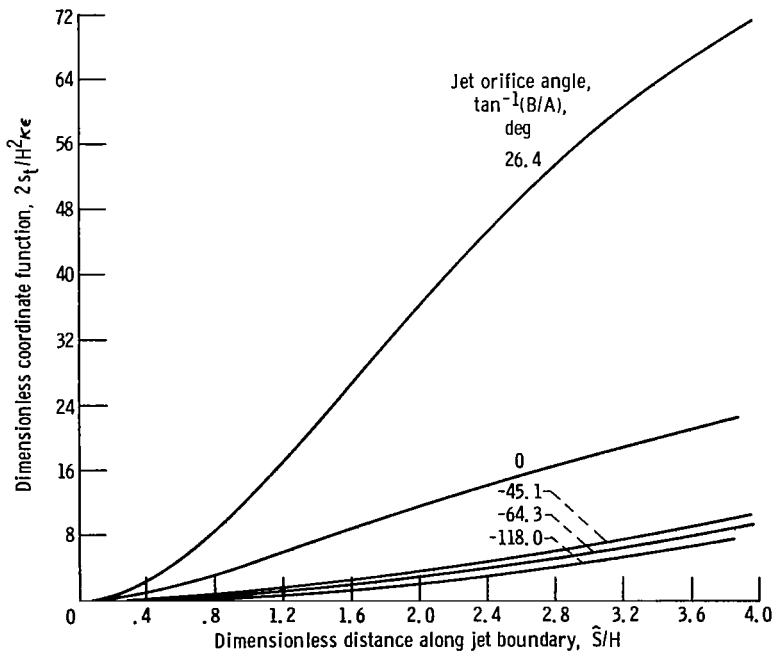


Figure 6. - Coordinate function for turbulent mixing of stream and separated jet.

nate  $s_t$  is presented as a function of  $\hat{S}$  for the separated and attached jets in figures 6 and 7, respectively. In each of the figures, curves are given for various orifice angles. The more complicated behavior of the attached jet curves at the larger orifice angle is the result of the complicated behavior of the slip line velocity which occurs in these cases (ref. 2).

Perhaps the most interesting quantities which can be obtained from the calculations are the mixing-region thicknesses  $\delta$  and  $\delta_t$ . The thicknesses for laminar mixing of

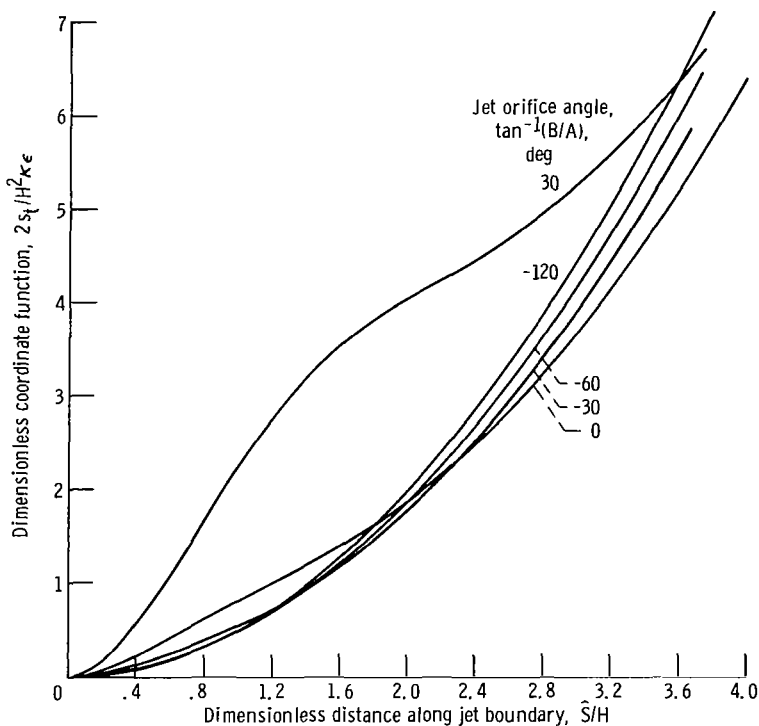


Figure 7. - Coordinate function for turbulent mixing of stream and attached jet.

the separated and attached jets are shown in figures 8 and 9. It can be seen from these figures that, at negative orifice angles for which the boundary between the jet and the mainstream is nearly a straight line and the flow in the jet and in the mainstream are almost parallel, the mixing-layer thickness grows as the square root of the distance  $\hat{S}$ . (Actually, it is easier to verify from figs. 4 and 5 that  $s$  varies linearly with  $\hat{S}$  for negative orifice angles and then use eq. (26) to establish that  $\delta$  varies as the square root of  $\hat{S}$ .) This behavior agrees with the well-known result that the thickness of the laminar mixing region between two parallel streams grows as the square root of the distance (ref. 6). Notice that  $\delta$  also depends on the square root of the Reynolds number which is characteristic of laminar flows.

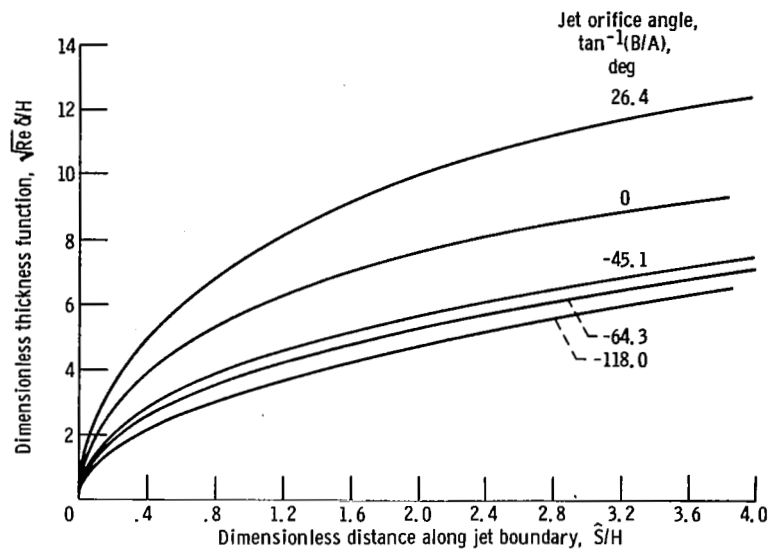


Figure 8. - Mixing-region thickness function for laminar mixing of stream and separated jet.

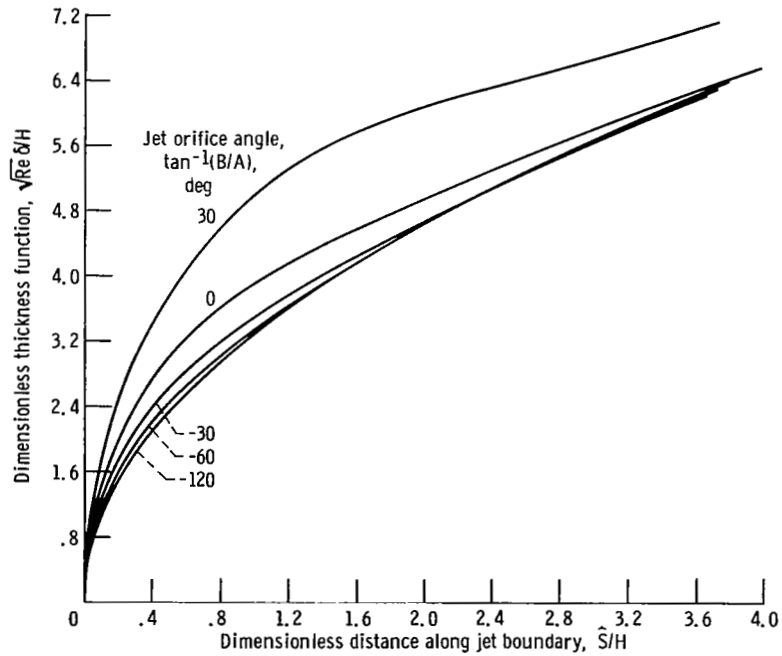


Figure 9. - Mixing-region thickness function for laminar mixing of stream and attached jet.

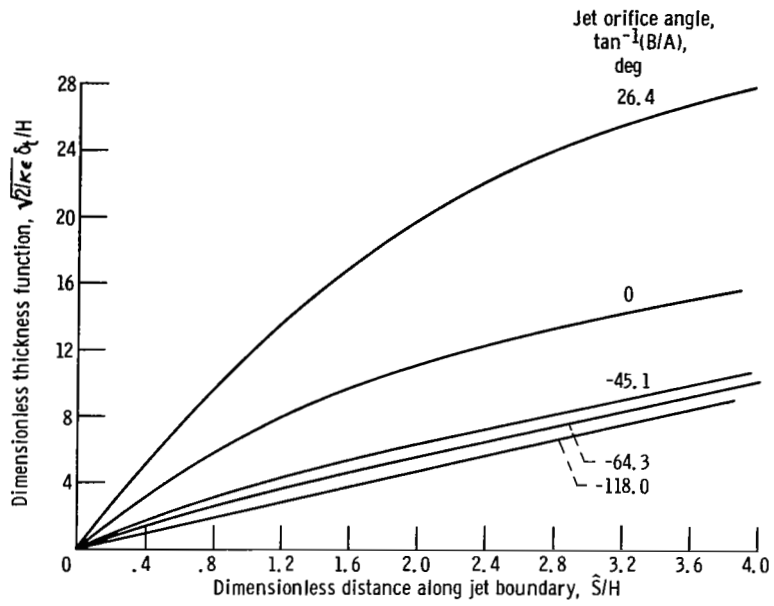


Figure 10. - Mixing-region thickness function for turbulent mixing of stream and separated jet.

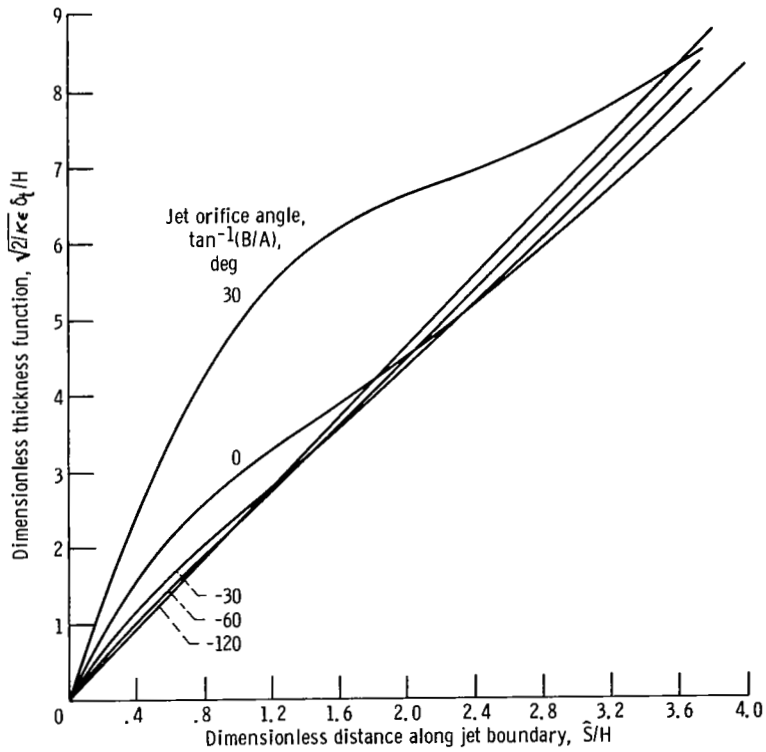


Figure 11. - Mixing-region thickness function for turbulent mixing of stream and attached jet.

In most cases of interest, the mixing region between the jet and the stream will be turbulent. The turbulent mixing-region thickness  $\delta_t$  is shown in figures 10 and 11 as a function of the distance along the slip line for the separated and attached jets, respectively. Again it can be seen from the figures that, at negative orifice angles for which the flow in the jet and in the main stream are nearly parallel, the mixing-layer thickness grows linearly with distance along the slip line. This behavior agrees with the well-known result that the thickness of the turbulent mixing region between two parallel streams grows linearly with distance. At positive orifice angles, the strong variations in velocity due to the bending of the streams cause the mixing-layer thickness to have a more complicated behavior. Notice that, just as in the case of parallel-stream mixing, the mixing-layer thickness is independent of Reynolds number and depends only on the parameter  $\sqrt{\kappa\epsilon}$ , where  $\kappa$  is an empirical constant related to the structure of the turbulence. A specific example of the way in which the velocity distribution along the jet boundary can affect the mixing-layer thickness is given in figure 12. In this figure, it

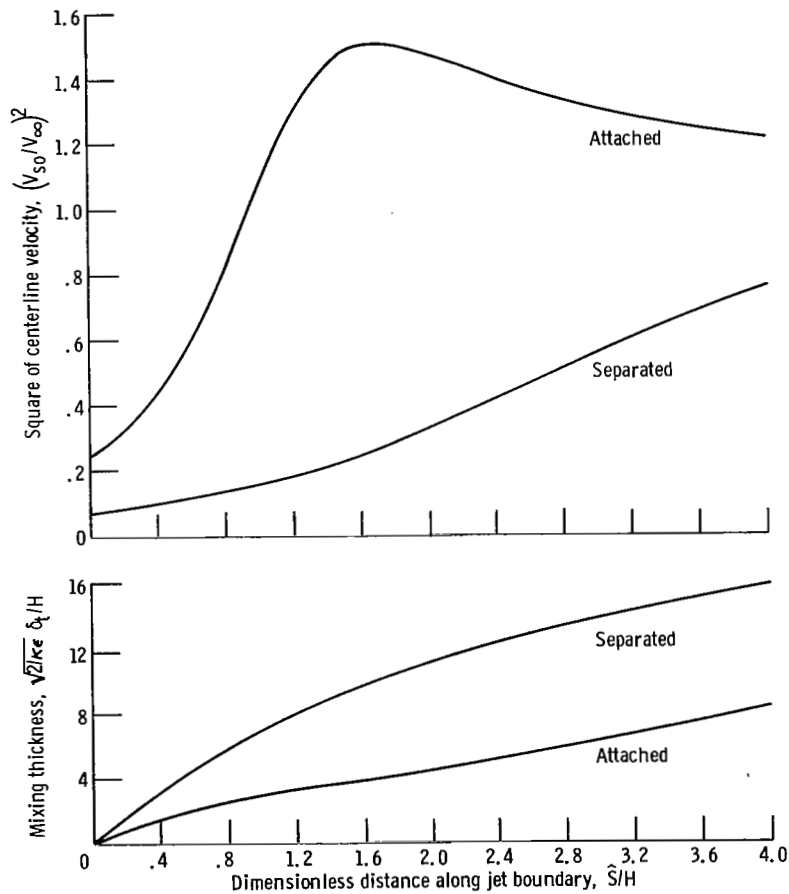


Figure 12. - Centerline velocity and breadth of turbulent mixing region. Jet orifice angle,  $\tan^{-1}(B/A)$ , 0.

has been assumed that the value of  $\kappa$  is the same as that for the mixing of parallel streams. The velocity ratio on the mixing-region centerline and the mixing-region thickness are plotted against distance along the slip line for both the attached and separated jets at zero orifice angle. Since the attached jet must turn much more abruptly than the separated jet, the velocity along the mixing region must attain much higher values in the former case. In fact, for the attached jet, the centerline velocity reaches a peak value in the region  $1 < \hat{S}/H < 2$ , which is considerably higher than the final jet velocity far downstream. In addition, the figure shows that, for the attached jet, the slowest rate of increase of mixing-layer thickness with distance also occurs in the region  $1 < \hat{S}/H < 2$ . The connection between these two phenomena can be explained in the following way. It has already been pointed out that for an observer moving with the centerline velocity of the mixing region, the mixing layer grows by a pure diffusion process. The diffusion rate is proportional to the velocity difference which in turn is inversely proportional to the centerline velocity across the mixing region (Prandtl's hypothesis). On the other hand, the distance moved by the observer along the slip line in a given time is proportional to the centerline velocity. Hence, if the centerline velocity of the mixing region is low, at a given point along the mixing region more outward diffusion will have occurred than if the centerline velocity were high.

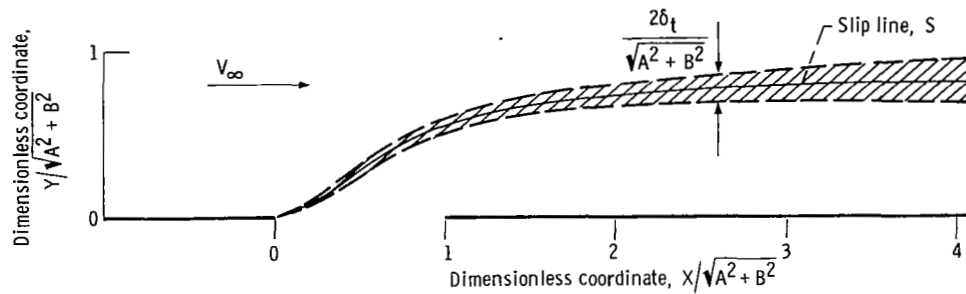


Figure 13. - Turbulent mixing region of attached jet and free stream. Jet orifice angle,  $\tan^{-1}(B/A)$ , 0;  $\epsilon = 0.2$ ;  $\kappa = 0.002$ ;  $H/\sqrt{A^2 + B^2} = 0.8563$ .

In figures 13 and 14, the mixing-layer thicknesses for the attached and separated jets, respectively, have been superimposed on plots of the jet contours. The centerline of the mixing region is taken to be the slip line obtained in references 1 and 2. (In ref. 5, comparison of theory and experiment shows that  $\kappa$  ranges from 0.00139 to 0.00251, so intermediate value  $\kappa = 0.002$  was chosen for the present calculations.)

The shaded areas represent the mixing regions. These plots correspond to a value of  $\epsilon$  of 0.2, which is near the upper limit of validity of the linearized theory presented in reference 2. Because of the small value of  $\epsilon$ , the mixing region grows relatively slowly with distance in the attached jet, but the fraction of the separated jet which is

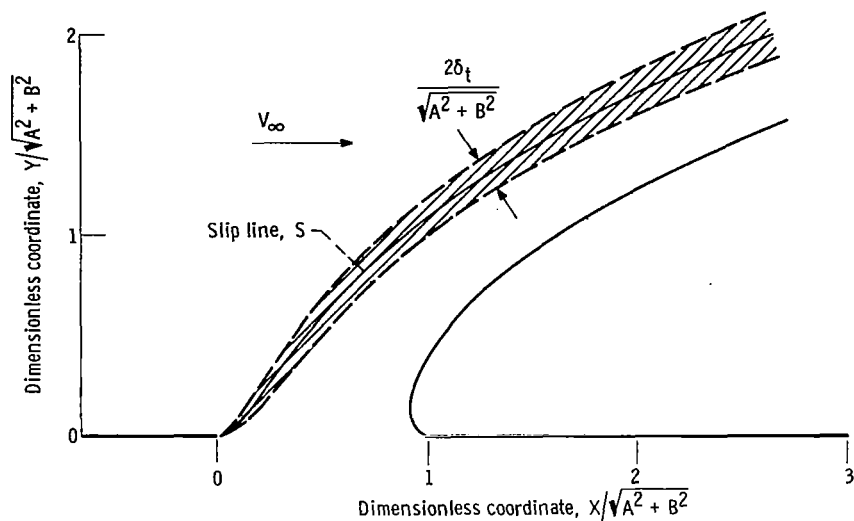


Figure 14. - Turbulent mixing region of separated jet and free stream. Jet orifice angle,  $\tan^{-1}(B/A)$ , 0;  $\epsilon = 0.2$ ;  $\kappa = 0.002$ ;  $H/\sqrt{A^2 + B^2} = 0.3240$ .

affected by the mixing is appreciable. In figure 13, the peak of velocity on the centerline occurs near

$$\frac{X}{\sqrt{A^2 + B^2}} = 1$$

In this discussion of the mixing of the jet and the stream, nothing has been said of the mixing of the separated jet with the stagnant wake, or the buildup of a boundary layer on the downstream wall of the orifice in the case of the attached jet. Both of these situations may be treated by existing techniques. In the case of a separated jet, the mixing region between the jet and the constant pressure wake region is the same as the mixing region between two parallel streams (ref. 6) under the assumption that the mixing-region thickness is always small compared with the radius of curvature of the free-stream line. The boundary layer on the downstream wall of the orifice, when the jet is attached, can be determined by using directly the usual techniques for calculating boundary layers in a pressure gradient (ref. 7). It is only necessary to know the velocity  $V$  external to the boundary layer. But this is given in reference 2 as a function of the distance from the lip  $\bar{X}$  in terms of a parameter  $\xi$  as

$$\frac{V}{V_{\infty}} = \frac{\xi}{\xi - \Delta}$$

$$\frac{X}{H} = \frac{1}{\pi} \left[ (\xi - \Delta) \left( 1 - \frac{1}{\xi} \right) + \frac{(1 - \Delta) \ln \xi}{\Delta} \right]$$

The quantity  $\Delta$  is given as a function of orifice angle in figure 8 of reference 2.

## CONCLUDING REMARKS

An analysis was made of the mixing region which occurs between a jet issuing from an orifice and a moving stream when the jet is injected at an oblique angle to the stream. The question of whether the jet is attached or separated is beyond the scope of the present analysis. The results show that, for the same conditions, the mixing region is thicker when the jet separates from the downstream edge of the orifice than when it remains attached. The analysis is performed by using boundary layer theory in conjunction with the results of inviscid solutions obtained previously.

Lewis Research Center,  
National Aeronautics and Space Administration,  
Cleveland, Ohio, August 26, 1969,  
129-01.

## APPENDIX - SYMBOLS

A	horizontal distance between edges of orifice	$V_s^-$	velocity on stream side of mixing region
B	vertical distance between edges of orifice	$v$	velocity in N-direction
H	asymptotic jet width	$v_1$	defined in eq. (6)
$H_0$	value of H to zero order in $\epsilon$	X, Y	Cartesian coordinates
J	defined in eq. (22c)	$\gamma$	variable of integration
K	defined in eq. (13)	$\Delta$	parameter related to orifice angle
N	coordinate normal to jet boundary	$\delta$	half thickness of laminar mixing region
O	order symbol (see eq. (5))	$\delta_t$	half thickness of turbulent mixing region
$P_j$	total pressure of jet	$\epsilon$	small parameter defined in eq. (1)
$P_\infty$	total pressure of stream	$\eta$	parametric variable
p	static pressure	$\kappa$	dimensionless proportionality constant for Prandtl's hypothesis
Re	Reynolds number, $H_0 V_\infty / \nu$	$\nu$	kinematic viscosity
S	slip line between jet and stream in inviscid solution	$\rho$	density of jet and stream
$\hat{S}$	distance along slip line	$\tau$	turbulent shear stress
$\hat{S}_0$	value of $\hat{S}$ to zero order in $\epsilon$	$\Omega^\pm$	first-order contributions to $V_s^\pm$ (eq. (2a))
$\hat{S}_1$	first-order contribution to $\hat{S}$		
s	defined in eq. (12)		
$s_t$	defined in eq. (19)		
T	defined in eq. (22b)		
u	velocity in $\hat{S}$ direction		
$u_1$	defined in eq. (5)		
$V_{s0}$	value of $V_s^+$ or $V_s^-$ to zero order in $\epsilon$		
$V_\infty$	free-stream velocity		
$V_s^+$	velocity on jet side of mixing region		

## REFERENCES

1. Goldstein, Marvin E. ; and Braun, Willis: Injection of an Inviscid Separated Jet at an Oblique Angle to a Moving Stream. NASA TN D-5460, 1969.
2. Goldstein, Marvin E. ; and Braun, Willis: Injection of an Attached Inviscid Jet at an Oblique Angle to a Moving Stream. NASA TN D-5501, 1969.
3. Goldstein, S., ed.: Modern Developments in Fluid Dynamics. Vol. I. Clarendon Press, Oxford, 1938, ch. 4.
4. Pai, Shih-i.: Fluid Dynamics of Jets. D. Van Nostrand Co., 1954, p. 112.
5. Mills, R. D.: Numerical and Experimental Investigations of the Shear Layer Between Two Parallel Streams. J. Fluid Mech., vol. 33, pt. 3, Sept. 2, 1968, pp. 591-616.
6. Ting, Lu: On the Mixing of Two Parallel Streams. J. Math. Phys., vol. 38, 1959, pp. 153-165.
7. Schlichting, Hermann (J. Kestin, trans.): Boundary-Layer Theory. Sixth ed., McGraw-Hill Book Co., Inc., 1968, chs. 10, 22.